Thin Solid Films 642 (2017) 14–19

Contents lists available at ScienceDirect

Thin Solid Films

journal homepage: www.elsevier.com/locate/tsf

Effect of precursor type and doping concentration on the physical properties of ultrasonically sprayed aluminium and indium co-doped zinc oxide thin films

Vinoth Kumar Jayaraman[a,*], Arturo Maldonado Álvarez[b], Monserrat Bizarro[a], Yuri Koudriavtsev[b], María de la Luz Olvera Amador[b]

[a] Instituto de Investigaciones en Materiales, Universidad Nacional Autónoma de México, México City, Mexico
[b] Departamento de Ingeniería Eléctrica-Sección de Estado Electrónico Sólido, Centro de Investigación y de Estudios Avanzados del Instituto Politécnico Nacional, México City, Mexico

ARTICLE INFO

Keywords:
AIZO
Aluminium chloride
Aluminium sulphate
Co-doping
Thin films
Optical properties
Ultrasonic spray pyrolysis
ZnO

ABSTRACT

In this work, we have studied the effect of aluminium dopant precursor type and doping concentration on the structural, morphological, optical and electrical properties of Al and In co-doped zinc oxide (AIZO) thin films deposited by ultrasonic spray pyrolysis. Zinc acetate dihydrate and indium acetate were used as zinc and indium precursors, respectively. Aluminium chloride and aluminium sulphate were used as aluminium precursors. The doping concentrations of Al (1 to 3 at%) and In (1 to 3 at%), were varied equally and the physical properties were analyzed. X-ray diffraction examinations confirmed that AIZO films were poly crystalline and grown as a hexagonal wurtzite structure. Scanning electron microscopy observations revealed that thin films were grown with different types of hexagonal nanostructures. From the optical and electrical measurements, the figure of merit was estimated. The values were $4.09 \times 10^{-3}/\Omega$ and $0.75 \times 10^{-3}/\Omega$ for the AIZO thin films deposited using aluminium chloride and aluminium sulphate respectively.

1. Introduction

Zinc oxide (ZnO) is an interesting semiconductor material which owns several special properties such as piezoelectric, pyroelectric, magnetic, resistance to radiation, and electrically conductive with an appropriate elemental doping [1–5]. In addition, ZnO is abundant, and inexpensive [6,7]. This multi-functionality behavior helps researchers to employ ZnO in various applications like actuators, memory devices, chemical gas sensors, thin films transistors, photo catalysis, energy storage devices and transparent conductive oxide (TCO) applications, among others [8–14]. From recent reports, we found that co-doping ZnO helps in improving the physical properties since undoped ZnO is highly resistive [15–17]. The electrical properties of a polycrystalline semiconductor are affected by different mechanisms such as free carrier scattering caused by impurities located in the grain boundaries and the value of the carrier concentration. In the literature, we found that, when metal ions ($Al^{3+}/In^{3+}/Ga^{3+}$) replaces Zn^{2+}, in turn increases the carrier concentration, thereby exhibits low resistivity provided that the dopants concentrations are below the solubility limit [18–21]. If doping is performed with excess concentrations, surplus atoms of dopants occupy the grain boundaries and results in high resistivity. This situation has been reported in Al doped ZnO thin films deposited by sol-gel, where authors mentioned that Al incorporates as Al_2O_3 aggregates at the ZnO grain boundaries [22]. Accordingly, under optimized deposition conditions, co-doping can be successful to decrease resistivity of ZnO thin films for TCO applications.

Though ZnO thin films can be prepared by many techniques such as thermal evaporation [23], sputtering [24], molecular beam epitaxy [25], pulsed laser deposition [26] etc., controlling the experimental parameters to achieve co-doped films with these techniques is a challenging process. In this regard, we have followed a chemical approach, ultrasonic spray pyrolysis (USP) to fabricate Al and In co-doped ZnO (AIZO) thin films. This technique offers several advantages such as simplicity, applicable for large-scale applications, cost and time effective [27–29]. The various experimental parameters involved in the deposition of thin films by USP are substrate temperature, solution concentration, dopants concentration, deposition time and solution flow rate [30–34]. However, for USP technique, the type of precursor salts may produce an impact in the properties of the material, but in the literature, no research has been found to investigate the effect of

* Corresponding author.
E-mail address: vinoth.jc@gmail.com (V.K. Jayaraman).

http://dx.doi.org/10.1016/j.tsf.2017.09.012
Received 19 October 2016; Received in revised form 31 August 2017; Accepted 8 September 2017
Available online 09 September 2017

precursor salts to produce AIZO thin films.

In this work, we have fabricated the AIZO thin films by varying the co-dopants concentrations and the type of Al precursor and investigated the physical characteristics such as structural, morphological, optical and electrical.

2. Experimental

Fabrication of Al and In co-doped zinc oxide thin films were performed on glass substrates by ultrasonic spray pyrolysis. Zn precursor solution of 0.2 M concentration was prepared from zinc acetate dihydrate ($Zn(OOCCH_3)_2{\cdot}2H_2O$, Alfa Aesar), using three solvents specifically acetic acid (5 ml), deionized water (5 ml) and methanol (90 ml). Aluminium dopant precursor solution was prepared using aluminium chloride ($AlCl_3{\cdot}6H_2O$, Alfa Aesar) of 0.1 M using methanol as a solvent and named as ALCL. One more aluminium dopant solution of 0.1 M was prepared by dissolving aluminium sulphate ($AlSO_4{\cdot}18H_2O$, Alfa Aesar) in methanol and named as ALS. Indium dopant solution of 0.2 M was prepared in an equal mixture of deionized water and acetic acid using indium acetate ($In(OOCCH_3)_3$, Alfa Aesar). Certain concentration of Al and In dopants were added in the Zn precursor solutions and growth of AIZO thin films were carried out by the deposition conditions as detailed in Table 1. In addition, an undoped ZnO thin film was prepared at 450 °C for 10 min using the Zn precursor solution to compare the figure of merit with co-doped films.

The structural characterization of the AIZO films was carried out with an X-ray diffractometer (PANalytical) with Cu K-alpha radiation. Thicknesses of the films were measured with a Bruker (Dektak) profilometer. High resolution morphologies were obtained by a Zeiss Auriga scanning electron microscope. Transmittance spectra were measured with a Shimadzu (Model no: 2401 PC) spectrophotometer. Sheet resistance values were gathered from a 4-point probe (Veeco) instrument. Thermogravimetric analysis (TGA) of aluminium salts was obtained using SDT Q600 V8.3 thermal analyzer. The existence of co-dopants was confirmed by depth analysis performed with ION TOF Secondary Ion Mass Spectroscopy (SIMS).

3. Results and discussion

3.1. Structural properties

The Fig. 1(a) shows the XRD patterns of thin films prepared using aluminium chloride precursor. Here we can observe that all the films are polycrystalline. The films ALCL-1 and ALCL-2 present (002) preferential orientation confirmed from texture co-efficient [35] estimations. In contrast, the film ALCL-3 show texture co-efficient near to 1 for many planes confirms that ALCL-3 is randomly oriented. Portillo-Vélez et al. also obtained ZnO thin films by spray pyrolysis with random orientation, when using a zinc acetate precursor [36].

The Fig. 1(b) shows the XRD diffraction patterns of the Al and In co-doped ZnO thin films fabricated using aluminium sulphate as Al precursor. No other notable peaks are found apart from (002) plane peak. All the ALS films show (002) as preferential orientation, in addition confirms the growth of hexagonal wurtzite structure [37,38]. The peaks

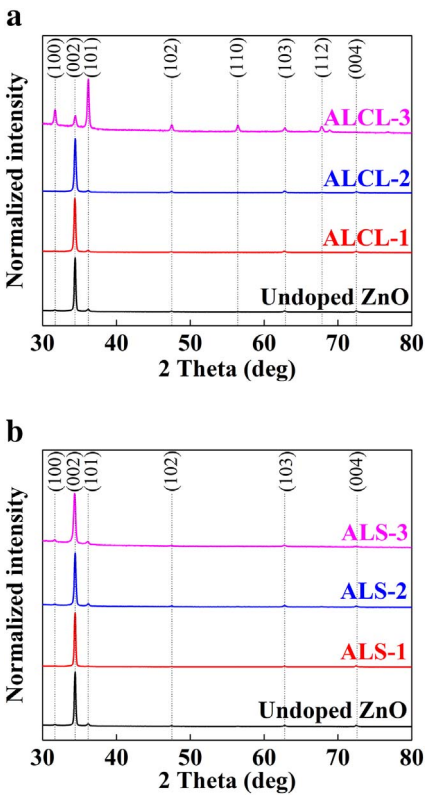

Fig. 1. (a). XRD of the AIZO thin films prepared using aluminium chloride as aluminium precursor and undoped ZnO thin film.
(b). XRD of the AIZO thin films prepared using aluminium sulphate as aluminium precursor and undoped ZnO thin film.

of the samples are slightly shifted from the undoped ZnO peak as well as the reference JCPDS file (01-089-0510). This shift might be attributed to tensile stress in the films [39]. In addition, peaks belonging to Al and In are not observed in the patterns, which confirms that the dopants are incorporated into the lattice of ZnO. Identically, Sin et al. reported that the absence of indium compounds in the indium doped ZnO thin films [40]. Further, films show a dominating peak along (002) plane indicating that AIZO thin films are grown along c-direction of wurtzite structure. However, there are variations in full width at half maximum (FWHM) with modifications in dopants concentration, which is a result of variation in thickness (t) (Table 2). Hence, the films ALCL-1 and ALS-1 show higher crystallinity than other films, since the films deposited with low dopants concentrations show low values of FWHM. The crystallite size and FWHM of the films are given in Table 2. The crystallite sizes (L) of the AIZO films (for the plane (002)) are estimated using Scherrer's formula $L = 0.9\lambda/\beta\cos\theta$ [41]

λ = wavelength, nm
β = FWHM, radians
θ = angle of diffraction, radians.

Table 1
AIZO thin film growth conditions.

Thin film ID	Al precursor ID	Al concentration (at%)	In concentration (at%)	Deposition time (min)	Deposition temperature (°C)
ALCL-1	ALCL	1	1	10	450
ALCL-2	ALCL	2	2	10	450
ALCL-3	ALCL	3	3	10	450
ALS-1	ALS	1	1	20	425
ALS-2	ALS	2	2	20	425
ALS-3	ALS	3	3	20	425

Table 2
Thickness and structural characteristics of the deposited films.

Thin film ID	Thickness (nm)	FWHM (deg)	Crystallite size (nm)
ALCL-1	690	0.1683	49.41
ALCL-2	447	0.2356	35.2
ALCL-3	461	0.2357	35.45 (for the plane (101))
ALS-1	763	0.1851	44.93
ALS-2	451	0.2019	41.19
ALS-3	265	0.3029	27.45
Undoped ZnO	439	0.1596	52.11

3.2. Morphological properties

The surface morphologies of the AIZO thin films and undoped ZnO obtained via scanning electron microscopy are shown in Fig. 2(a–h).

ALCL-1 film presents grains with hexagonal plate shape morphology that tends to pile up (Fig. 2a). The sizes of the structures vary in between ~50 to 350 nm. However, when dopants concentration increases, ALCL-2 (Fig. 2b) shows a surface with isolated hexagonal plates with a size distribution of ~100–400 nm. Further increase in dopants concentration (Fig. 2c) destroys the hexagonal shape and results in compact leaves-like structures. Fig. 2(a,b,c) clearly shows that as co-dopants concentrations increases, compactness also increases in film surface.

When AIZO films are prepared using aluminium sulphate, the film morphologies are appeared as in Fig. 2(d,e,f). Hexagonal plate structures over which screwed pyramidal structures are formed when the co-dopants concentration is very low (1 at%) of size ~200 to 400 nm. Inclusion of 2 at% of co-dopants results in the formation of either hexagonal plates or irregular features. Addition of 3 at% of co-dopants leads to the growth of hexagonal flakes and few triangles of different sizes from ~180 nm to 400 nm. The undoped ZnO thin films showed a morphology with irregular hexagons (Fig. 2(g–h)). The size distribution

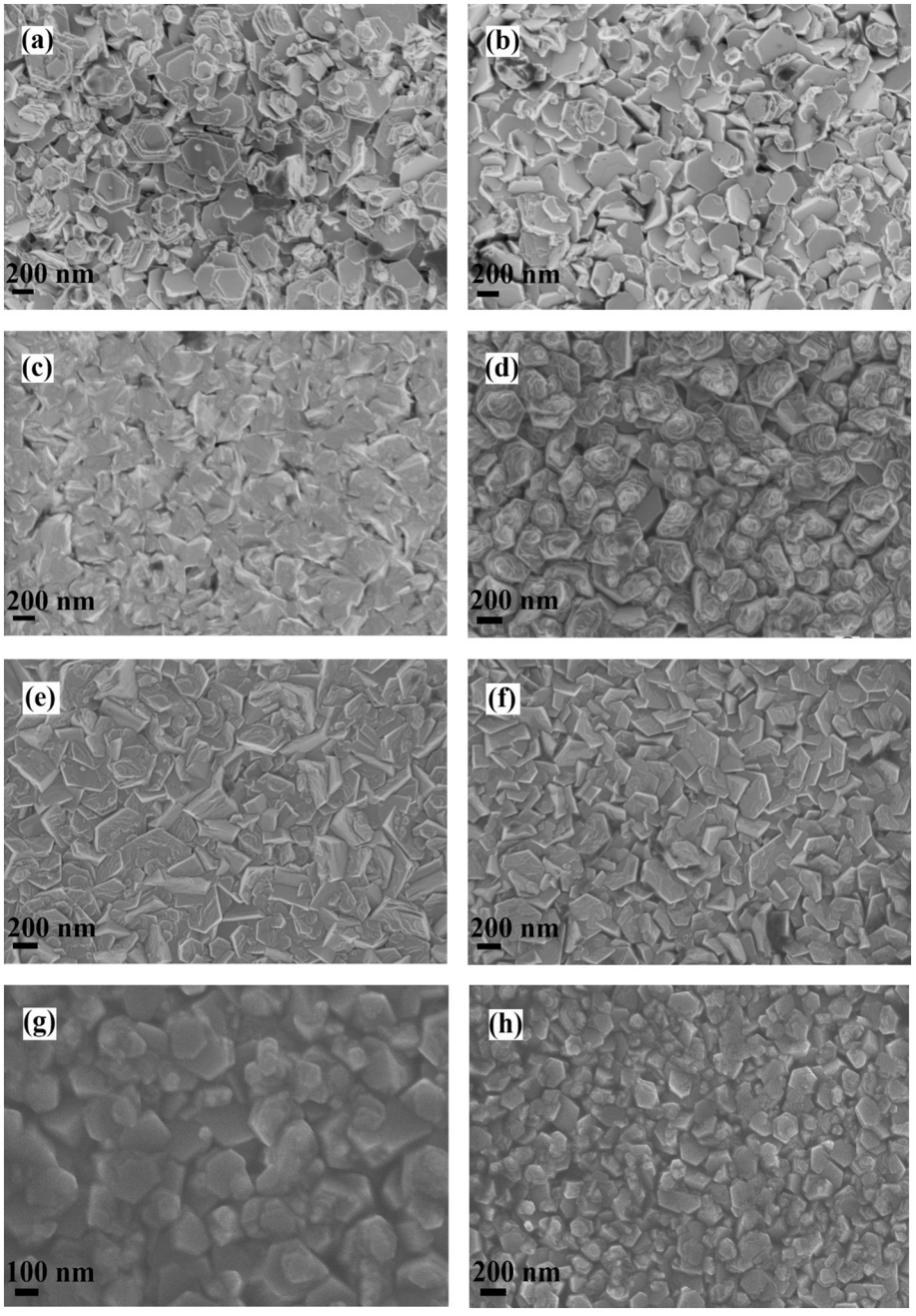

Fig. 2. Thin film morphologies of (a) ALCL-1, (b) ALCL-2, (c) ALCL-3, (d) ALS-1, (e) ALS-2, (f) ALS-3, (g) Undoped ZnO at 50 KX magnification, and (h) Undoped ZnO at 25 KX magnification.

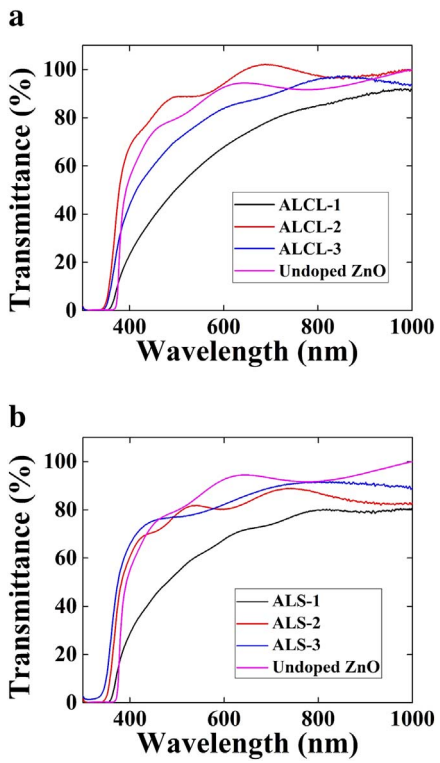

Fig. 3. (a). Optical transmittance of the AIZO thin films prepared using aluminium chloride as aluminium precursor and undoped ZnO thin film.
(b). Optical transmittance of the AIZO thin films prepared using aluminium sulphate as aluminium precursor and undoped ZnO thin film.

of the hexagons is found to be in between 100 and 210 nm.

3.3. Optical and electrical properties

Fig. 3a shows the transmittance of deposited undoped and co-doped thin films prepared using aluminium chloride as an aluminium precursor. From the Table 3 we can observe that there is a drastic change in transmittance values, which is a result of change in thickness (Table 2).

Fig. 3b shows the transmittance of undoped ZnO, ALS-1, ALS-2 and ALS-3 films. ALS-3 presents the lower transmittance than ALS-2, though the thickness is low for ALS-3. This behavior could be due to type of nanostructure formed on the thin film surface.

When we compare Fig. 3a and b following discussions can be concluded:

a) Films doped with low concentration result in very low transmittances.
b) In both cases, films co-doped with 2 at% show high transmittances (> 80%).
c) The bandgap (E_g) values are found to be oscillating between 3.41 and 3.48 eV. However, E_g is slightly upwards shifted from the undoped ZnO (Eg = 3.31 eV), this can be due to an increase in carrier concentration, which is called Burstein-Moss effect [42].

Table 3
Optical and electrical parameters of undoped ZnO and AIZO thin films.

Thin film ID	T_{550} (%)	E_g (eV)	R_s (Ω/□)	ρ ($\times 10^{-3}$Ω-cm)	Figure of Merit (FOM) (10^{-3}/Ω)
ALCL-1	59.96	3.42	79	5.45	0.07
ALCL-2	89.10	3.41	77	3.44	4.09
ALCL-3	77.85	3.41	152	7.00	0.53
ALS-1	61.58	3.48	72	5.49	0.11
ALS-2	81.17	3.44	164	7.39	0.75
ALS-3	78.79	3.41	309	8.18	0.29
Undoped ZnO	86.17	3.31	38 K	1668.20	0.006

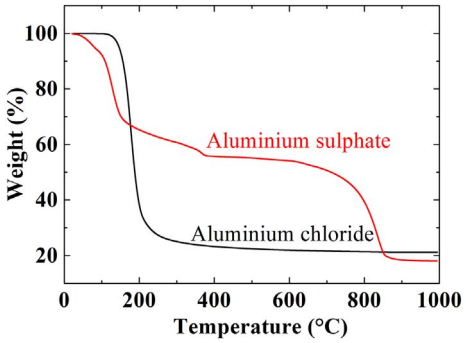

Fig. 4. Thermogravimetric analysis of aluminium precursors.

In addition, when we observe electrical characteristics from Table 3, all the films show resistivity ($\rho = R_s * t$) in the order of 10^{-3}Ω-cm, lower than undoped ZnO resistivity which in turn assures that co-dopants are well-substituted into the Zn lattice, in turn would have increased the carrier concentration.

The factors that affect the electro-optical characteristics are type of dopant, composition of elements and the deposition environment. To evaluate the figure of merit (Φ_{TC}), Haacke's formula ($\Phi_{TC} = T^{10}/R_s$, where T is the transmittance at 550 nm and R_s is the sheet resistance) is employed [43]. The film ALCL-2 appears to be the best since it shows the highest figure of merit (4.09×10^{-3}/Ω), could be due to the better decomposition of aluminium chloride than aluminium sulphate, which was confirmed from TGA plots. Fig. 4 shows the TGA plots of the aluminium precursors, where 77% of weight loss occurs for aluminium chloride at 425 °C, whereas it is only 45% for aluminium sulphate at 450 °C. It is worth to mention that we performed several preliminary studies on deposition times and temperatures (between 400 and 475 °C) to obtain high values of figure of merit. We found that 10 min deposition at 425 °C is the excellent condition while using aluminium chloride and 20 min deposition at 450 °C is the optimum condition while using aluminium sulphate as aluminium precursor. In addition, the achieved FOM is quite competitive with the reported FOM in the literature (in between 1.74×10^{-6} and 8.47×10^{-3}/Ω) for the extrinsic ZnO thin films deposited by ultrasonic spray pyrolysis [44–47].

Fig. 5(a) & (b) shows the depth profile of the samples ALCL-2 and ALS-2 obtained by SIMS, where the thin films contain the elements Zn, O, In and Al. The average atomic concentration of Zn, O, In, and Al for ALCL-2 film are 1.50×10^{22}, 1.68×10^{22}, 4.64×10^{20}, and 3.62×10^{19} atoms/cm^3 respectively. Similarly, for ALS-2 the obtained concentration values of Zn, O, In, and Al are 1.98×10^{22}, 1.87×10^{22}, 5.29×10^{20}, and 2.30×10^{18} atoms/cm^3 respectively.

4. Conclusions

Aluminium and indium co-doped zinc oxide (AIZO) thin films were grown on glass substrates by ultrasonic spray pyrolysis. The structural, morphological, optical and electrical properties were investigated with changes in precursor type and co-dopants concentration in the spraying solution. Investigation on structural properties showed that films were crystalline and no evidence of Al_2O_3 or In_2O_3 were observed. Morphological studies showed that AIZO films result in different morphological when there were changes in the experimental conditions. Optical and electrical measurements indicated that films grown using aluminium chloride as an Al dopant precursor exhibited the highest figure of merit ~4.09×10^{-3}/Ω. Thus, our results prove that choosing an appropriate precursor and doping concentration are important factors in obtaining films for the suitability of transparent conductive oxide applications.

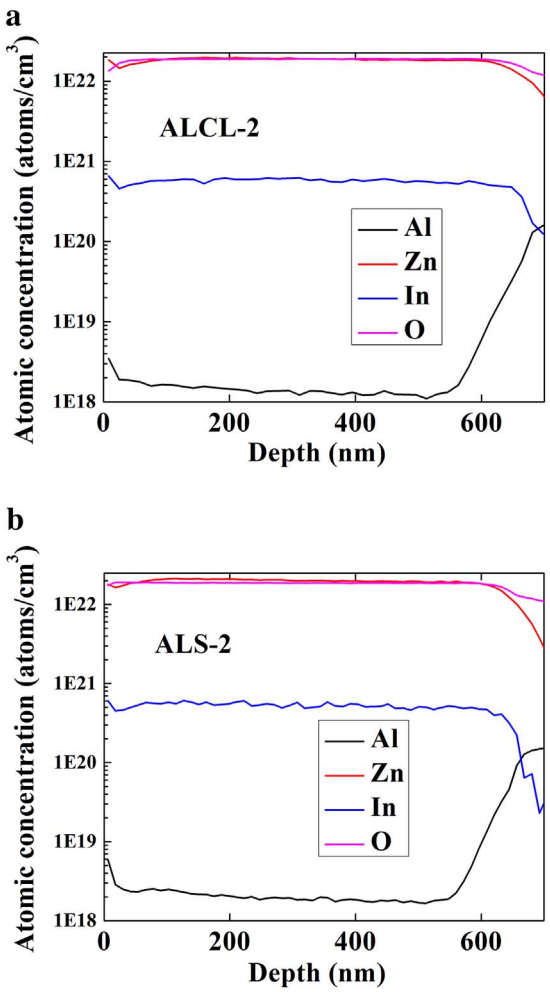

Fig. 5. (a). SIMS elemental depth profile of AIZO thin film (ALCL-2) prepared using aluminium chloride.
(b). SIMS elemental depth profile of AIZO thin film (ALS-2) prepared using aluminium sulphate.

Acknowledgments

The authors thank A. Palafox, M. A. Luna-Arias, N. Iris, A. Tavira, J. Roque (LANE) and K. E. Morales (IIM) for their help in technical characterization. Vinoth is grateful to UNAM-DGAPA for postdoctoral fellowship. This project funding is partially supported by UNAM-PAPIIT-IN106015.

References

[1] W.W. Qin, Y.T. Li, T. Li, J.W. Qiu, X.J. Ma, D. Wei, X. Chen, X.F. Hu, W. Zhang, Microstructure-related piezoelectric properties of a ZnO film grown on a Si substrate, Ceram. Int. 42 (2016) 16927–16934, http://dx.doi.org/10.1016/j.ceramint.2016.07.192.
[2] C.C. Hsiao, Y.C. Hu, R.C. Chang, C.K. Chao, Residual stresses and mechanical properties of a ZnO pyroelectric sensor, Theor. Appl. Fract. Mech. 52 (2009) 1–6, http://dx.doi.org/10.1016/j.tafmec.2009.06.002.
[3] S.C. Chen, C.H. Wang, H. Sun, C.K. Wen, C.F. Lu, C.L. Tsai, Y.K. Fu, T.H. Chuang, Microstructures, electrical and magnetic properties of (Ga, Co)-ZnO films by radio frequency magnetron co-sputtering, Surf. Coat. Technol. 303 (2016) 203–208, http://dx.doi.org/10.1016/j.surfcoat.2016.03.064.
[4] M.J.F. Empizo, K. Yamanoi, K. Mori, K. Iwano, Y. Iwasa, Y. Minami, R. Arita, K. Fukuda, K. Takano, T. Shimizu, M. Nakajima, M. Yoshimura, N. Sarukura, T. Norimatsu, M. Hangyo, H. Azechi, T. Fukuda, B.G. Singidas, R.V. Sarmago, M. Oya, Y. Ueda, Optical damage assessment and recovery investigation of hydrogen-ion and deuterium-ion plasma-irradiated bulk ZnO single crystals, J. Appl. Phys. 121 (2017), http://dx.doi.org/10.1063/1.4982346.
[5] D. Das, P. Mondal, Low temperature grown ZnO:Ga films with predominant c-axis orientation in wurtzite structure demonstrating high conductance, transmittance and photoluminescence, RSC Adv. 6 (2016) 6144–6153, http://dx.doi.org/10.1039/C5RA22288E.
[6] M.I. Khan, K.A. Bhatti, R. Qindeel, L.G. Bousiakou, N. Alonizan, Fazal-e-Aleem, investigations of the structural, morphological and electrical properties of multilayer ZnO/TiO_2 thin films, deposited by sol-gel technique, Results Phys. 6 (2016) 156–160, http://dx.doi.org/10.1016/j.rinp.2016.01.015.
[7] K. Minder, F.H. Teherani, D. Rogers, C. Bayram, R. McClintock, P. Kung, M. Razeghi, Etching of ZnO towards the development of ZnO homostructure LEDs, Proc. SPIE Vol 6474 (2007) 64740Q, http://dx.doi.org/10.1117/12.712784.
[8] Y. Yuan, K. Shyong Chow, H. Du, P. Wang, M. Zhang, S. Yu, B. Liu, A ZnO thin-film driven microcantilever for nanoscale actuation and sensing, Int. J. Smart Nano Mater. 4 (2013) 128–141, http://dx.doi.org/10.1080/19475411.2012.749959.
[9] N.M. Muhammad, N. Duraisamy, K. Rahman, H.W. Dang, J. Jo, K.H. Choi, Fabrication of printed memory device having zinc-oxide active nano-layer and investigation of resistive switching, Curr. Appl. Phys. 13 (2013) 90–96, http://dx.doi.org/10.1016/j.cap.2012.06.017.
[10] R. Kumar, O. Al-Dossary, G. Kumar, A. Umar, Zinc oxide nanostructures for NO_2 gas-sensor applications: a review, Nano-Micro Lett. 7 (2015) 97–120, http://dx.doi.org/10.1007/s40820-014-0023-3.
[11] A.M. Ma, M. Gupta, F.R. Chowdhury, M. Shen, K. Bothe, K. Shankar, Y. Tsui, D.W. Barlage, Zinc oxide thin film transistors with Schottky source barriers, Solid State Electron. 76 (2012) 104–108, http://dx.doi.org/10.1016/j.sse.2012.05.005.
[12] K.M. Lee, C.W. Lai, K.S. Ngai, J.C. Juan, Recent developments of zinc oxide based photocatalyst in water treatment technology: a review, Water Res. 88 (2016) 428–448, http://dx.doi.org/10.1016/j.watres.2015.09.045.
[13] V. Cauda, D. Pugliese, N. Garino, A. Sacco, S. Bianco, F. Bella, A. Lamberti, C. Gerbaldi, Multi-functional energy conversion and storage electrodes using flower-like zinc oxide nanostructures, Energy 65 (2014) 639–646, http://dx.doi.org/10.1016/j.energy.2013.12.025.
[14] F.Z. Ghomrani, A. Aissat, H. Arbouz, A. Benkouider, Al concentration effect on ZnO based thin films: for photovoltaic applications, Energy Procedia 74 (2015) 491–498, http://dx.doi.org/10.1016/j.egypro.2015.07.733.
[15] S.D. Kirby, R.B. van Dover, Improved conductivity of ZnO through codoping with in and Al, Thin Solid Films 517 (2009) 1958–1960, http://dx.doi.org/10.1016/j.tsf.2008.10.066.
[16] A. Elfakir, T.S. Tlemçani, E.B. Benamar, A. Belayachi, E. Gutierrez-Berasategui, G. Schmerber, M. Balestrieri, S. Colis, A. Slaoui, A. Dinia, M. Abd-Lefdil, Structural, electrical and optical properties of sprayed Nd–F codoped ZnO thin films, J. Sol-Gel Sci. Technol. 73 (2015) 557–562, http://dx.doi.org/10.1007/s10971-014-3518-y.
[17] M.S. Tokumoto, A. Smith, C. Santilli, S.H. Pulcinelli, A.F. Craievich, E. Elkaim, A. Traverse, V. Briois, Structural electrical and optical properties of undoped and indium doped ZnO thin films prepared by the pyrosol process at different temperatures, Thin Solid Films 416 (2002) 284–293, http://dx.doi.org/10.1016/S0040-6090(02)00531-X.
[18] A.R. Babar, P.R. Deshamukh, R.J. Deokate, D. Haranath, C.H. Bhosale, K.Y. Rajpure, Gallium doping in transparent conductive ZnO thin films prepared by chemical spray pyrolysis, J. Phys. D. Appl. Phys. 41 (2008) 135404, http://dx.doi.org/10.1088/0022-3727/41/13/135404.
[19] S. Benramache, O. Belahssen, H. Ben Temam, Effect of band gap energy on the electrical conductivity in doped ZnO thin film, J. Semicond. 35 (2014) 73001, http://dx.doi.org/10.1088/1674-4926/35/7/073001.
[20] F. Maldonado, A. Stashans, Al-doped ZnO: Electronic, electrical and structural properties, J. Phys. Chem. Solids 71 (2010) 784–787, http://dx.doi.org/10.1016/j.jpcs.2010.02.001.
[21] G. MacHado, D.N. Guerra, D. Leinen, J.R. Ramos-Barrado, R.E. Marotti, E.A. Dalchiele, Indium doped zinc oxide thin films obtained by electrodeposition, Thin Solid Films 490 (2005) 124–131, http://dx.doi.org/10.1016/j.tsf.2005.04.042.
[22] D.C. Altamirano-Juárez, G. Torres-Delgado, S. Jiménez-Sandoval, O. Jiménez-Sandoval, R. Castanedo-Pérez, Low-resistivity ZnO:F:Al transparent thin films, Sol. Energy Mater. Sol. Cells 82 (2004) 35–43, http://dx.doi.org/10.1016/j.solmat.2004.01.003.
[23] O.A. Fouad, A.A. Ismail, Z.I. Zaki, R.M. Mohamed, Zinc oxide thin films prepared by thermal evaporation deposition and its photocatalytic activity, Appl. Catal. B Environ. 62 (2006) 144–149, http://dx.doi.org/10.1016/j.apcatb.2005.07.006.
[24] V.K. Jayaraman, Y.M. Kuwabara, A.M. Álvarez, M.D.L.L.O. Amador, Importance of substrate rotation speed on the growth of homogeneous ZnO thin films by reactive sputtering, Mater. Lett. 169 (2016) 1–4, http://dx.doi.org/10.1016/j.matlet.2016.01.088.
[25] E. Przezdziecka, W. Lisowski, R. Jakiela, J.W. Sobczak, A. Jablonski, M.A. Pietrzyk, A. Kozanecki, Arsenic chemical state in MBE grown epitaxial ZnO layers – doped with As, N and Sb, J. Alloys Compd. 687 (2016) 937–942, http://dx.doi.org/10.1016/j.jallcom.2016.06.213.
[26] P. Liang, H. Cai, X. Yang, H. Li, W. Zhang, N. Xu, J. Sun, J. Wu, Spectroscopic characterization of the plasmas formed during the deposition of ZnO and Al-doped ZnO films by plasma-assisted pulsed laser deposition, Spectrochim. Acta B At. Spectrosc. 125 (2016) 18–24, http://dx.doi.org/10.1016/j.sab.2016.09.003.
[27] J.V. Kumar, A. Maldonado, M. Olvera, A simple and cost-effective zinc oxide thin film sensor for propane gas detection, Mater. Lett. 157 (2015) 169–171, http://dx.doi.org/10.1016/j.matlet.2015.05.065.
[28] D. Paraguay, L. Estrada, N. Acosta, E. Andrade, M. Miki-Yoshida, Growth, structure and optical characterization of high quality ZnO thin films obtained by spray pyrolysis, Thin Solid Films 350 (1999) 192–202, http://dx.doi.org/10.1016/S0040-6090(99)00050-4.
[29] B.J. Babu, A. Maldonado, S. Velumani, Deposition and Characterization of ZnO: Al Thin Films by Ultrasonic Spray Pyrolysis, 6th Int. Conf. Electr. Eng. Comput. Sci. Autom. Control, (2009), http://dx.doi.org/10.1109/ICEEE.2009.5393563.

[30] S. Benramache, B. Benhaoua, Influence of substrate temperature and Cobalt concentration on structural and optical properties of ZnO thin films prepared by Ultrasonic spray technique, Superlattice. Microst. 52 (2012) 807–815, http://dx.doi.org/10.1016/j.spmi.2012.06.005.
[31] V. Mata, A. Maldonado, M.D.L.L. Olvera, Effect of precursor concentration in the starting solution on the photocatalytic activity of ZnO thin films, 2015 12th Int. Conf. Electr. Eng. Comput. Sci. Autom. Control. CCE 2015, 2015, pp. 1–4, , http://dx.doi.org/10.1109/ICEEE.2015.7358001.
[32] L.-C. Chen, C.-A. Hsieh, X. Zhang, Electrical properties of CZO films prepared by ultrasonic spray pyrolysis, Materials (Basel). 7 (2014) 7304–7313, http://dx.doi.org/10.3390/ma7117304.
[33] V.K. Jayaraman, A. Maldonado-Alvarez, A.E. Jimenez-Gonzalez, M.D.L.L. Olvera-Amador, Influence of precursor ball milling in enhancing the structural, morphological, optical and electrical properties of AIZO thin films, Mater. Lett. 181 (2016) 52–55, http://dx.doi.org/10.1016/j.matlet.2016.06.007.
[34] Y. Benkhetta, A. Attaf, H. Saidi, A. Bouhdjar, H. Benjdidi, I.B. Kherchachi, M. Nouadji, N. Lehraki, Influence of the solution flow rate on the properties of zinc oxide (ZnO) nano-crystalline films synthesized by ultrasonic spray process, Opt. Int. J. Light Electron Opt. 127 (2016) 3005–3008, http://dx.doi.org/10.1016/j.ijleo.2015.11.236.
[35] M. Kumar, A. Kumar, A.C. Abhyankar, Influence of texture coefficient on surface morphology and sensing properties of W-doped nanocrystalline tin oxide thin films, ACS Appl. Mater. Interfaces 7 (2015) 3571–3580, http://dx.doi.org/10.1021/am507397z.
[36] N.S. Portillo-Vélez, M. Bizarro, Sprayed pyrolyzed ZnO films with nanoflake and nanorod morphologies and their photocatalytic activity, J. Nanomater. 5981562 (2016), http://dx.doi.org/10.1155/2016/5981562.
[37] F.K. Allah, S.Y. Abé, C.M. Núñez, A. Khelil, L. Cattin, M. Morsli, J.C. Bernède, A. Bougrine, M.A. del Valle, F.R. Díaz, Characterisation of porous doped ZnO thin films deposited by spray pyrolysis technique, Appl. Surf. Sci. 253 (2007) 9241–9247, http://dx.doi.org/10.1016/j.apsusc.2007.05.055.
[38] K. Bahedi, M. Addou, M. El Jouad, S. Bayoud, Z. Sofiani, Effects of deposition temperature on the surface roughness and the nonlinear optical susceptibility of sprayed deposited ZnO:Zr thin films, Appl. Surf. Sci. 255 (2009) 9054–9057, http://dx.doi.org/10.1016/j.apsusc.2009.06.104.
[39] M. Anusha, D. Arivuoli, High intense violet luminescence in fluorine doped zinc oxide (FZO) thin films deposited by aerosol assisted CVD, J. Alloys Compd. 580 (2013) 131–136, http://dx.doi.org/10.1016/j.jallcom.2013.05.073.
[40] S.Y. Lim, S. Brahma, C.P. Liu, R.C. Wang, J.L. Huang, Effect of indium concentration on luminescence and electrical properties of indium doped ZnO nanowires, Thin Solid Films 549 (2013) 165–171, http://dx.doi.org/10.1016/j.tsf.2013.09.001.
[41] P.M.R. Kumar, C.S. Kartha, K.P. Vijayakumar, T. Abe, Y. Kashiwaba, F. Singh, D.K. Avasthi, On the properties of indium doped ZnO thin films, Semicond. Sci. Technol. 20 (2005) 120–126, http://dx.doi.org/10.1088/0268-1242/20/2/003.
[42] A.P. Roth, J.B. Webb, D.F. Williams, Band-gap narrowing in heavily defect-doped ZnO, Phys. Rev. B 25 (1982) 7836–7839, http://dx.doi.org/10.1103/PhysRevB.25.7836.
[43] G. Haacke, New figure of merit for transparent conductors, J. Appl. Phys. 47 (1976) 4086–4089, http://dx.doi.org/10.1063/1.323240.
[44] A.G. Fedoseev, N.A. Lashkova, L.B. Matyushkin, ZnO and Aluminium Doped ZnO Thin Films Synthesis by Ultrasonic Spray Pyrolysis Technique, (2017), pp. 1391–1393, http://dx.doi.org/10.1109/EIConRus.2017.7910829.
[45] R.R. Biswal, A. Maldonado, M.D.L. Olvera, Electrical and Optical Properties of In-doped ZnO Thin Films via Ultrasonic Spray Pyrolysis, (2013), pp. 407–410, http://dx.doi.org/10.1109/ICEEE.2013.6676014.
[46] P. Arnou, J.W. Bowers, J.M. Walls, Aluminium-doped zinc oxide deposited by ultrasonic spray pyrolysis for thin film solar cell applications, IEEE Photovoltaic Specialists Conference, 2014, http://dx.doi.org/10.1109/PVSC.2014.6924920.
[47] V. Kumar, A.M. Álvarez, Y.M. Kuwabara, Y. Koudriavstev, M.D. Olvera, Effect of co-doping concentration on structural, morphological, optical and electrical properties of aluminium and indium co-doped ZnO thin films deposited by ultrasonic spray pyrolysis, Mater. Sci. Semicond. Process. 47 (2016) 32–36, http://dx.doi.org/10.1016/j.mssp.2016.02.011.